Supplementary Materials

PhyMLP: an automated strategy for machine-learning potential construction via data fusion and adaptive point-sampling

Yiqun Guo[1,#], Shihui Ning[2,#], Guoqi Guo[2], Yangchun Chen[2,*], Bowen Huang[2,*], Shifang Xiao[1,*], Wangyu Hu[2,*]

[1]School of Physics and Electronics, Hunan University, Changsha 410082, Hunan, China.
[2]College of Materials Science and Engineering, Hunan University, Changsha 410082, Hunan, China.
[#]Authors contributed equally.

[*]**Correspondence to:** Dr. Shifang Xiao, School of Physics and Electronics, Hunan University, Changsha 410082, Hunan, China. E-mail: shifangxiao@hnu.edu.cn; Dr. Yangchun Chen, Dr. Bowen Huang, Prof. Wangyu Hu, College of Materials Science and Engineering, Hunan University, Changsha 410082, Hunan, China. E-mail: ychchen@hnu.edu.cn; bowen_huang@hnu.edu.cn; wyuhu@hnu.edu.cn

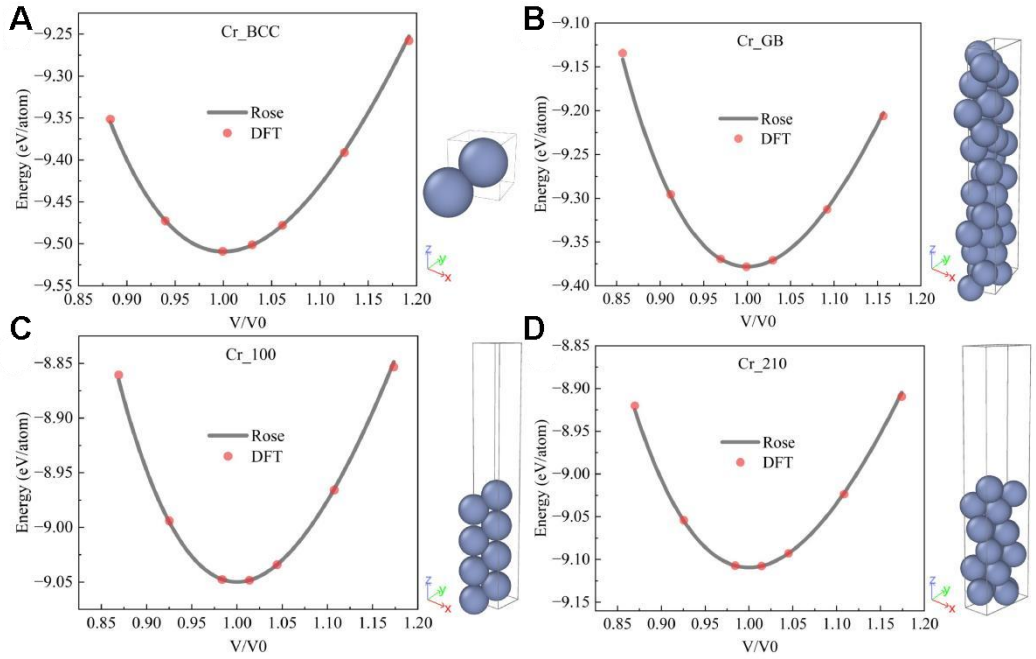

Supplementary Figure 1. Comparison of the energy-volume scaling relationships for Cr configurations calculated by the Rose equation and reference DFT methods. The horizontal axes show the relative volume (V/V0), and the vertical axes represent the energy (eV/atom). (A) BCC standard structure of Cr. (B) Grain boundaries of Cr. (C) (100) surface of Cr. (D) (210) surface of Cr. [The data for the structures come from the Materials Project, ID: mp-90/mp-8633.]

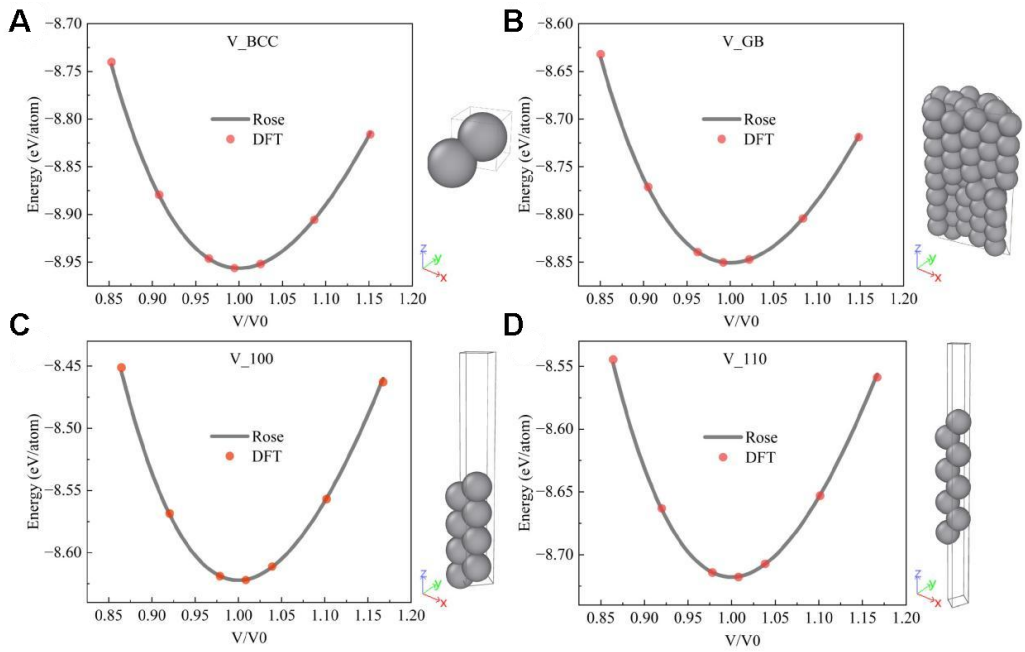

Supplementary Figure 2. Comparison of the energy-volume scaling relationships for V configurations calculated by the Rose equation and reference DFT methods. The horizontal axes show the relative volume (V/V0), and the vertical axes represent the energy (eV/atom). (A) BCC standard structure of V. (B) Grain boundaries of V. (C) (100) surface of V. (D) (110) surface of V. [The data for the structures come from the Materials Project, ID: mp-146/mp-8632.]

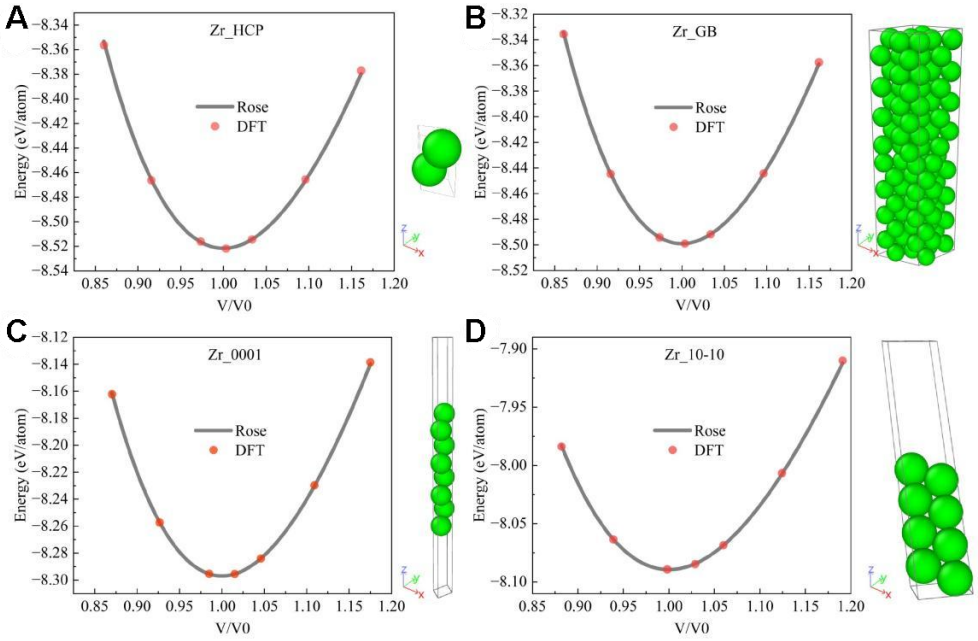

Supplementary Figure 3. Comparison of the energy-volume scaling relationships for Zr configurations calculated by the Rose equation and reference DFT methods. The horizontal axes show the relative volume (V/V0), and the vertical axes represent the energy (eV/atom). (A) HCP standard structure of Zr. (B) Grain boundaries of Zr. (C) (0001) surface of Zr. (D) (10-10) surface of Zr. [The data for the structures come from the Materials Project, ID: mp-41/mp-131/mp-8635.]

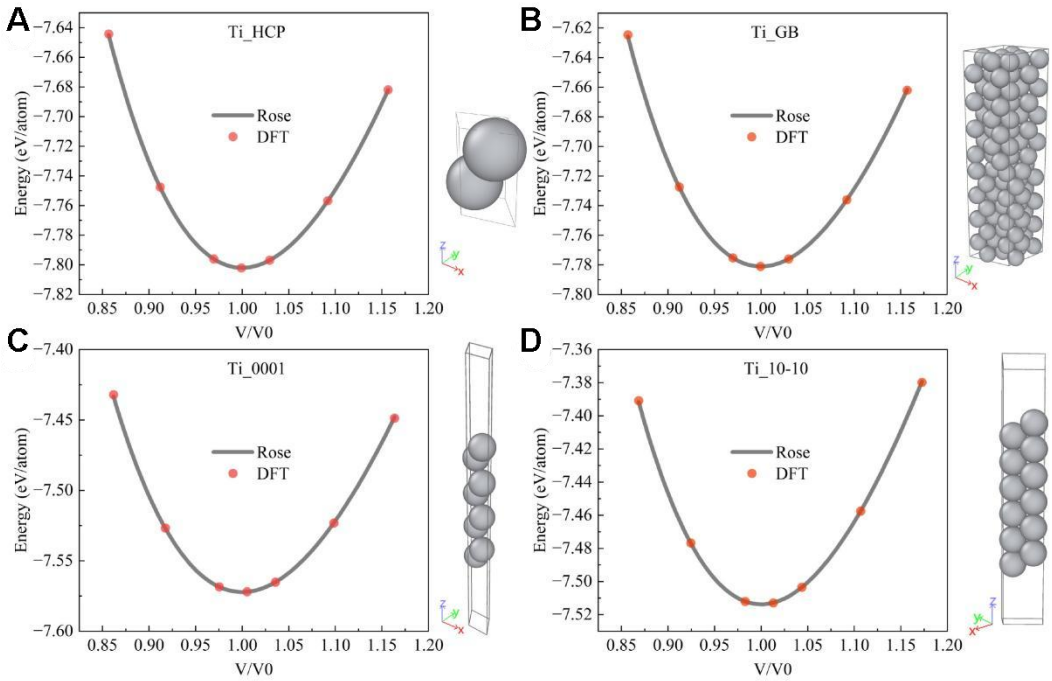

Supplementary Figure 4. Comparison of the energy-volume scaling relationships for Ti configurations calculated by the Rose equation and reference DFT methods. The horizontal axes show the relative volume (V/V0), and the vertical axes represent the energy (eV/atom). (A) HCP standard structure of Ti. (B) Grain boundaries of Ti. (C) (0001) surface of Ti. (D) (10-10) surface of Ti. [The data for the structures come from the Materials Project, ID: mp-46/mp-73/mp-6985.]

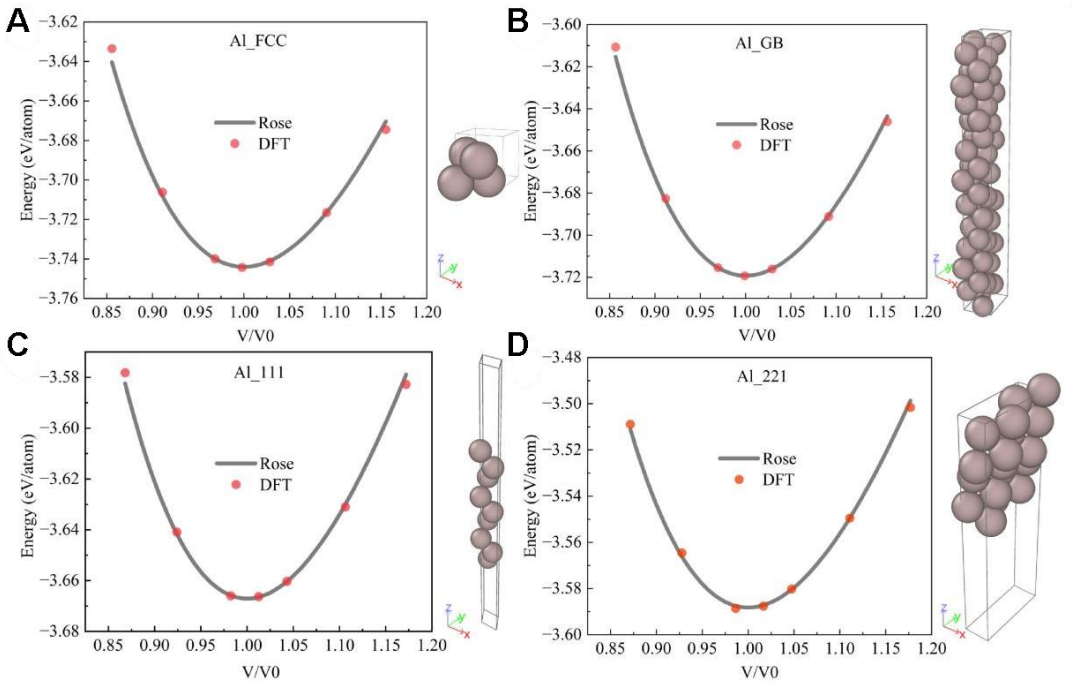

Supplementary Figure 5. Comparison of the energy-volume scaling relationships for Al configurations calculated by the Rose equation and reference DFT methods. The horizontal axes show the relative volume (V/V0), and the vertical axes represent the energy (eV/atom). (A) BCC standard structure of Al. (B) Grain boundaries of Al. (C) (111) surface of Al. (D) (221) surface of Al. [The data for the structures come from the Materials Project, ID: mp-134.]

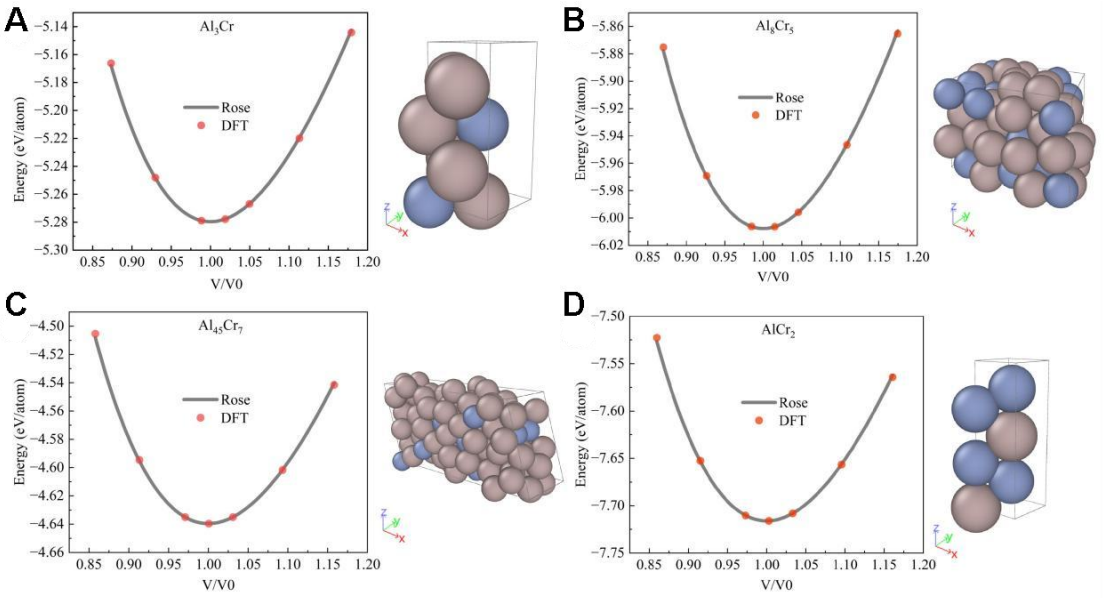

Supplementary Figure 6. Comparison of the energy-volume scaling relationships for Al-Cr configurations calculated by the Rose equation and reference DFT methods. The horizontal axes show the relative volume (V/V0), and the vertical axes represent the energy (eV/atom). (A) Al_3Cr configuration. (B) Al_8Cr_5 configuration. (C) $Al_{45}Cr_7$ configuration. (D) $AlCr_2$ configuration. [The data for the structures come from the Materials Project, ID: mp-867780/mp-19954/mp-31019/mp-1699.]

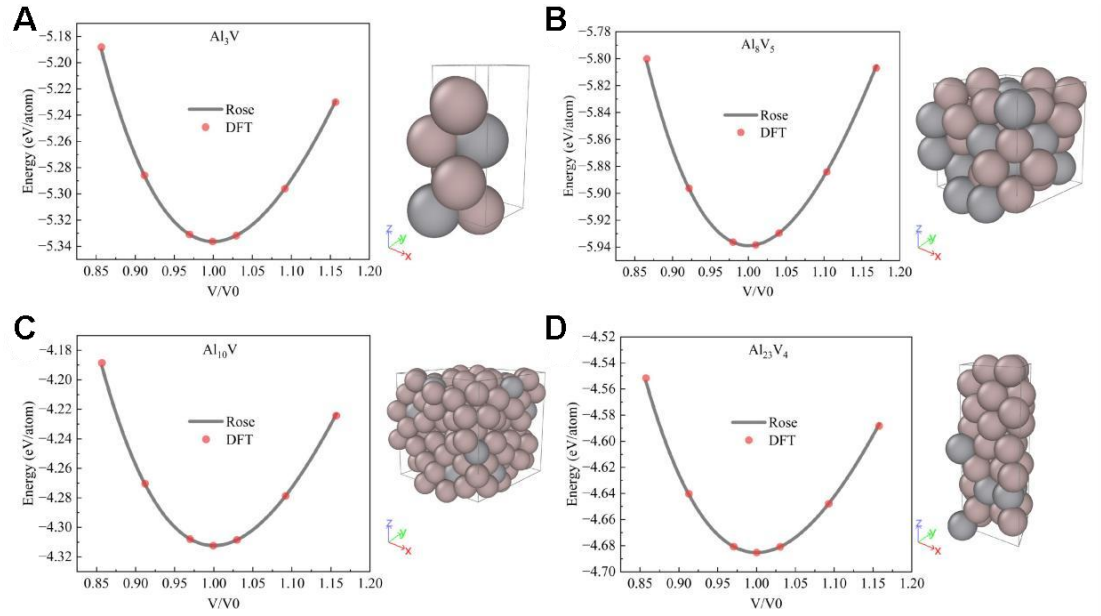

Supplementary Figure 7. Comparison of the energy-volume scaling relationships for Al-V configurations calculated by the Rose equation and reference DFT methods. The horizontal axes show the relative volume (V/V0), and the vertical axes represent the energy (eV/atom). (A) Al_3V configuration. (B) Al_8V_5 configuration. (C) $Al_{10}V$ configuration. (D) $Al_{23}V_4$ configuration. [The data for the structures come from the Materials Project, ID: mp-2554/mp-1008554/mp-30335 etc.]

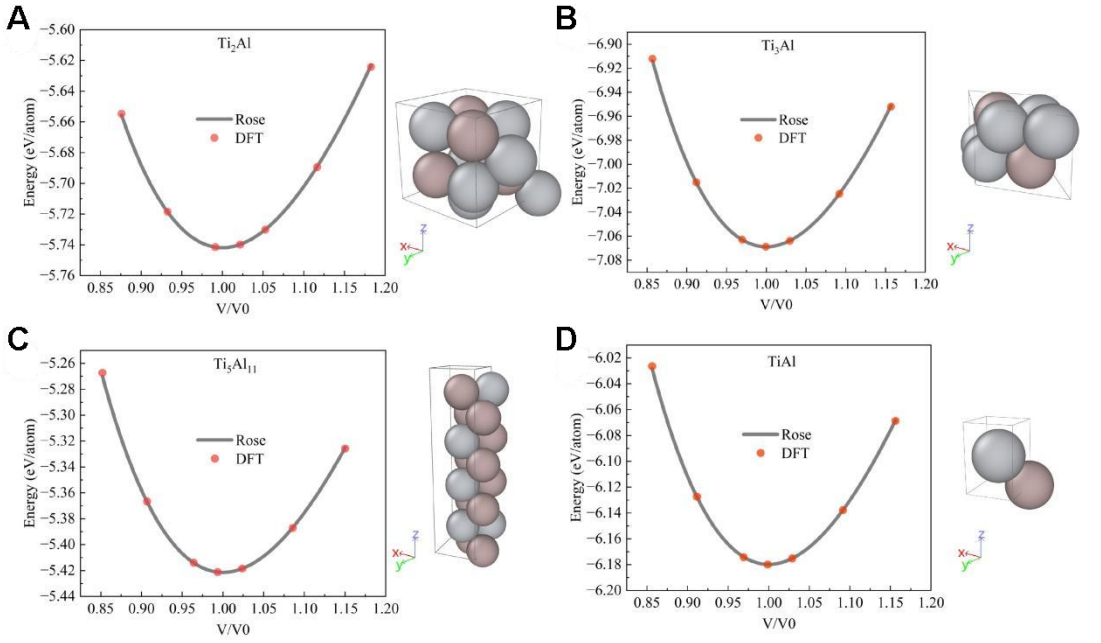

Supplementary Figure 8. Comparison of the energy-volume scaling relationships for Ti-Al configurations calculated by the Rose equation and reference DFT methods. The horizontal axes show the relative volume (V/V0), and the vertical axes represent the energy (eV/atom). (A) Ti_2Al configuration. (B) Ti_3Al configuration. (C) Ti_5Al_{11} configuration. (D) TiAl configuration. [The data for the structures come from the Materials Project, ID: mp-1823/mp-1953/mp-1008753 etc.]

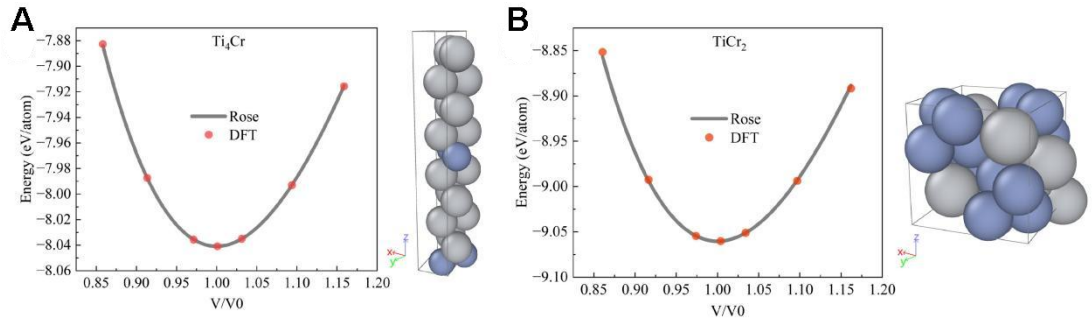

Supplementary Figure 9. Comparison of the energy-volume scaling relationships for Ti-Cr configurations calculated by the Rose equation and reference DFT methods. The horizontal axes show the relative volume (V/V0), and the vertical axes represent the energy (eV/atom). (A) Ti_4Cr configuration. (B) $TiCr_2$ configuration. [The data for the structures come from the Materials Project, ID: mp-1425/mp-1589/mp-1217156 etc.]

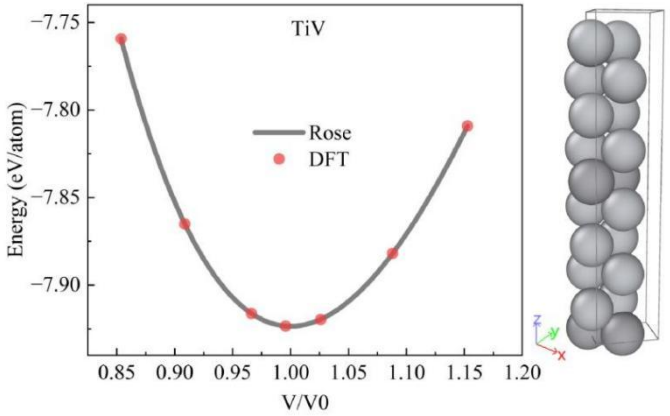

Supplementary Figure 10. Comparison of the energy-volume scaling relationships for TiV configurations calculated by the Rose equation and reference DFT methods. The horizontal axes show the relative volume (V/V0), and the vertical axes represent the energy (eV/atom). [The data for the structures come from the Materials Project, ID: mp-1217117/mp-1216646.]

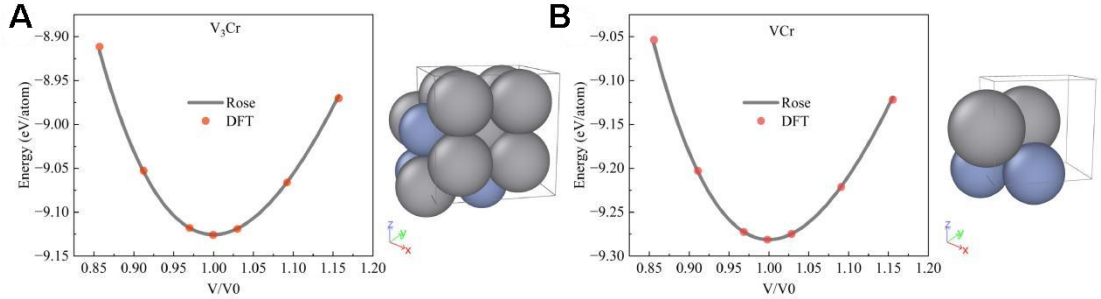

Supplementary Figure 11. Comparison of the energy-volume scaling relationships for V-Cr configurations calculated by the Rose equation and reference DFT methods. The horizontal axes show the relative volume (V/V0), and the vertical axes represent the energy (eV/atom). (A) V_3Cr configuration. (B) VCr configuration. [The data for the structures come from the Materials Project, ID: mp-1187695/mp-1216394/mp-1187696.]

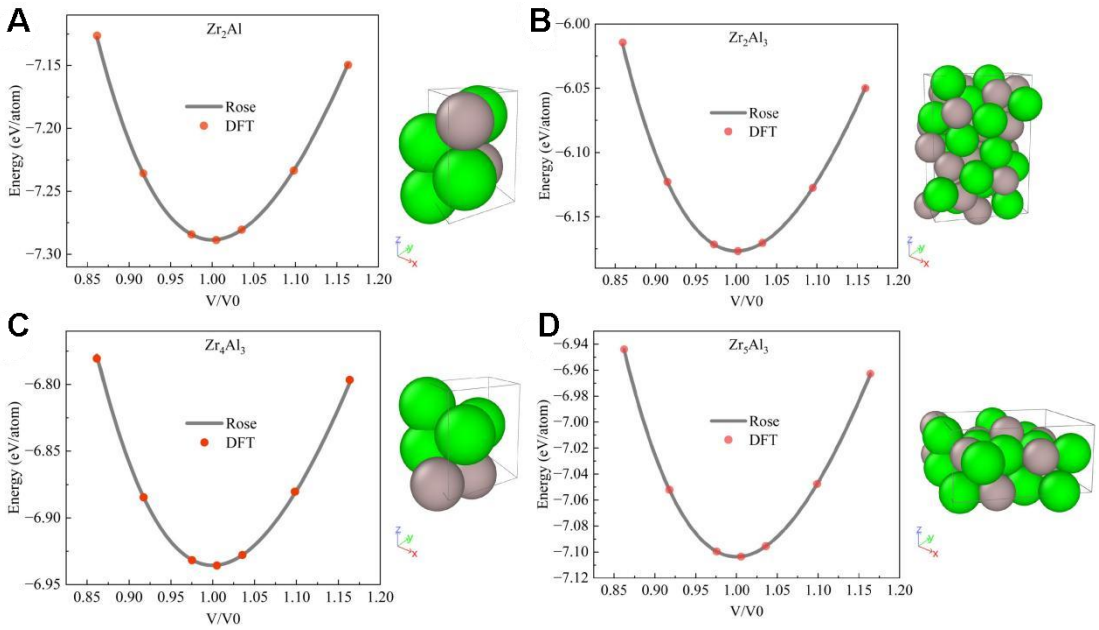

Supplementary Figure 12. Comparison of the energy-volume scaling relationships for Zr-Al configurations calculated by the Rose equation and reference DFT methods. The horizontal axes show the relative volume (V/V0), and the vertical axes represent the energy (eV/atom). (A) Zr_2Al configuration. (B) Zr_2Al_3 configuration. (C) Zr_4Al_3 configuration. (D) Zr_5Al_3 configuration. [The data for the structures come from the Materials Project, ID: mp-2557/mp-12773/mp-1471 etc.]

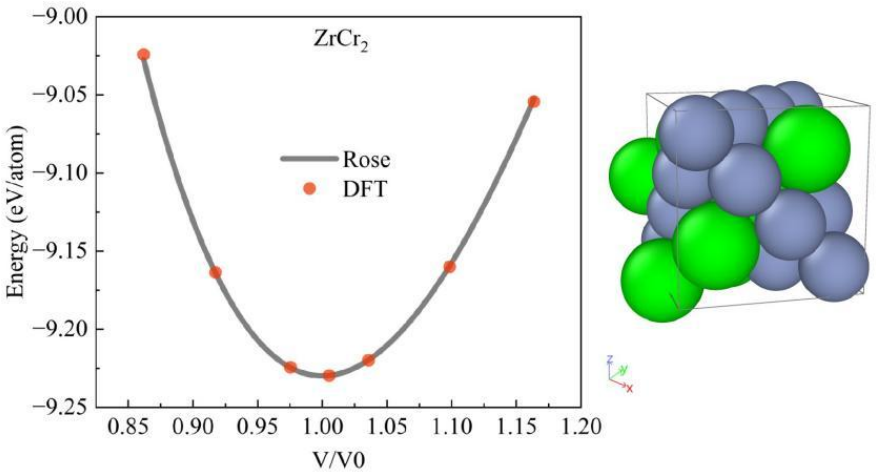

Supplementary Figure 13. Comparison of the energy-volume scaling relationships for $ZrCr_2$ configurations calculated by the Rose equation and reference DFT methods. The horizontal axes show the relative volume (V/V0), and the vertical axes represent the energy (eV/atom). [The data for the structures come from the Materials Project, ID: mp-903/mp-1919/mp-570608.]

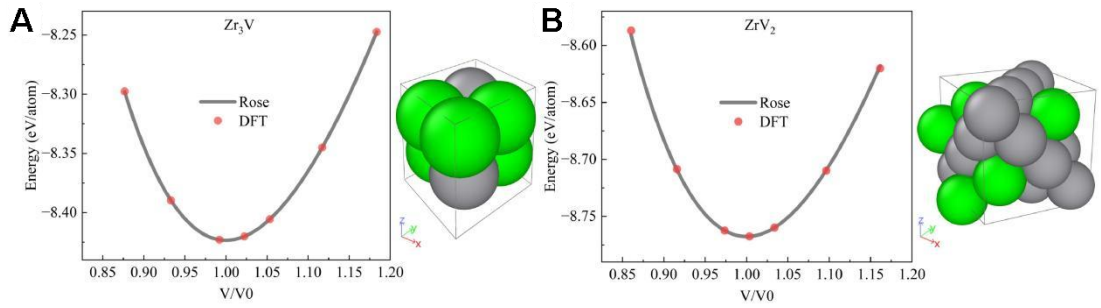

Supplementary Figure 14. Comparison of the energy-volume scaling relationships for Zr-V configurations calculated by the Rose equation and reference DFT methods. The horizontal axes show the relative volume (V/V0), and the vertical axes represent the energy (eV/atom). (A) Zr_3V configuration. (B) ZrV_2 configuration. [The data for the structures come from the Materials Project, ID: mp-1188058/mp-258.]

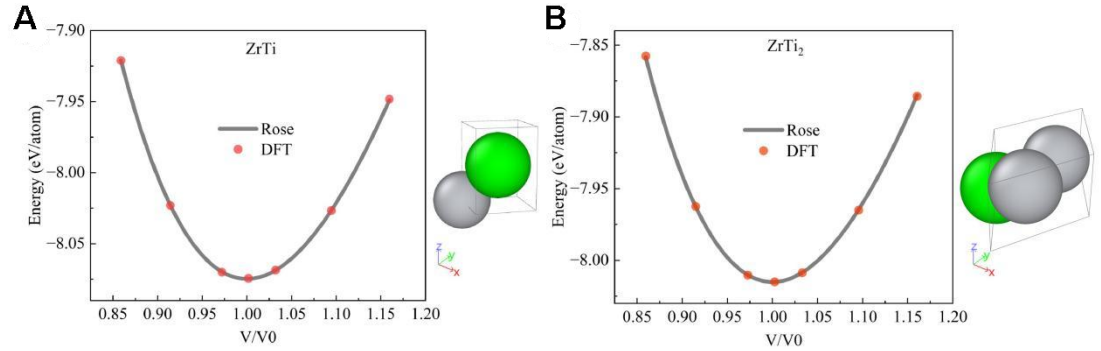

Supplementary Figure 15. Comparison of the energy-volume scaling relationships for Zr-Ti configurations calculated by the Rose equation and reference DFT methods. The horizontal axes show the relative volume (V/V0), and the vertical axes represent the energy (eV/atom). (A) ZrTi configuration. (B) $ZrTi_2$ configuration. [The data for the structures come from the Materials Project, ID: mp-1215200/mp-1215236/mp-1008568 etc.]

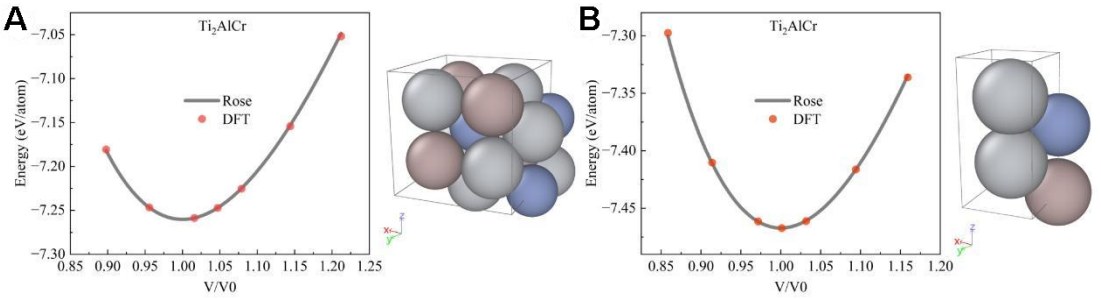

Supplementary Figure 16. Comparison of the energy-volume scaling relationships for Ti-Al-Cr configurations calculated by the Rose equation and reference DFT methods. The horizontal axes show the relative volume (V/V0), and the vertical axes represent the energy (eV/atom). (A) Ti_2AlCr configuration. (B) Ti_2AlCr another configuration. [The data for the structures come from the Materials Project, ID: mp-999096/mp-1217087.]

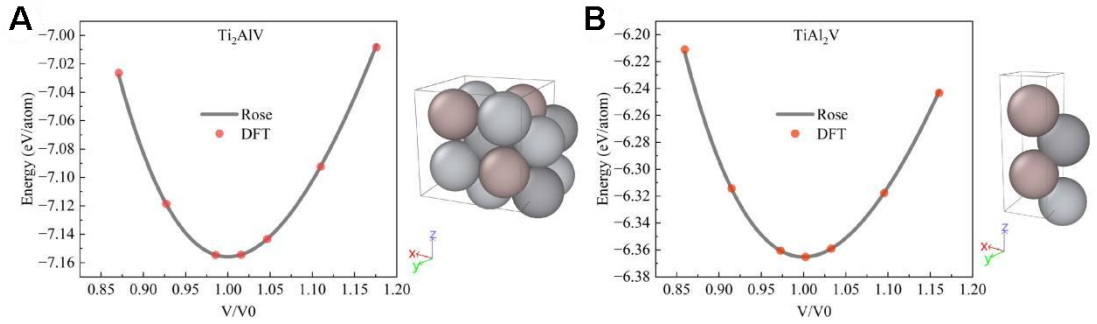

Supplementary Figure 17. Comparison of the energy-volume scaling relationships for Ti-Al-V configurations calculated by the Rose equation and reference DFT methods. The horizontal axes show the relative volume (V/V0), and the vertical axes represent the energy (eV/atom). (A) Ti_2AlV configuration. (B) $TiAl_2V$ configuration. [The data for the structures come from the Materials Project, ID: mp-999068/mp-1217015/mp-1217032.]

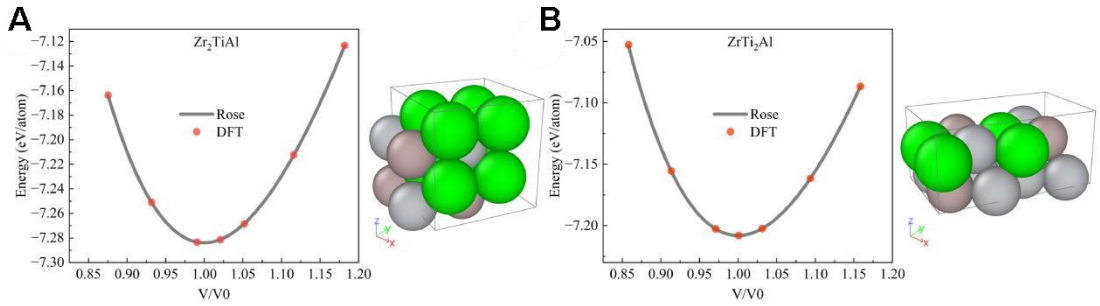

Supplementary Figure 18. Comparison of the energy-volume scaling relationships for Zr-Ti-Al configurations calculated by the Rose equation and reference DFT methods. The horizontal axes show the relative volume (V/V0), and the vertical axes represent the energy (eV/atom). (A) Zr_2TiAl configuration. (B) $ZrTi_2Al$ configuration. [The data for the structures come from the Materials Project, ID: mp-1064892/mp-1215242.]

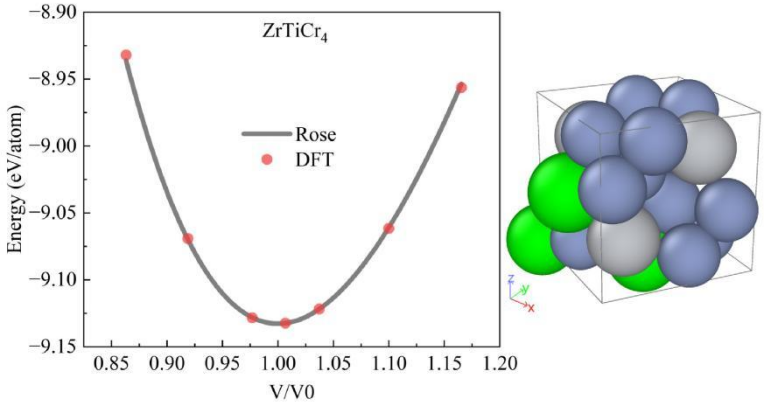

Supplementary Figure 19. Comparison of the energy-volume scaling relationships for $ZrTiCr_4$ configurations calculated by the Rose equation and reference DFT methods. The horizontal axes show the relative volume (V/V0), and the vertical axes represent the energy (eV/atom). [The data for the structures come from the Materials Project, ID: mp-1215179/mp-1215221.]

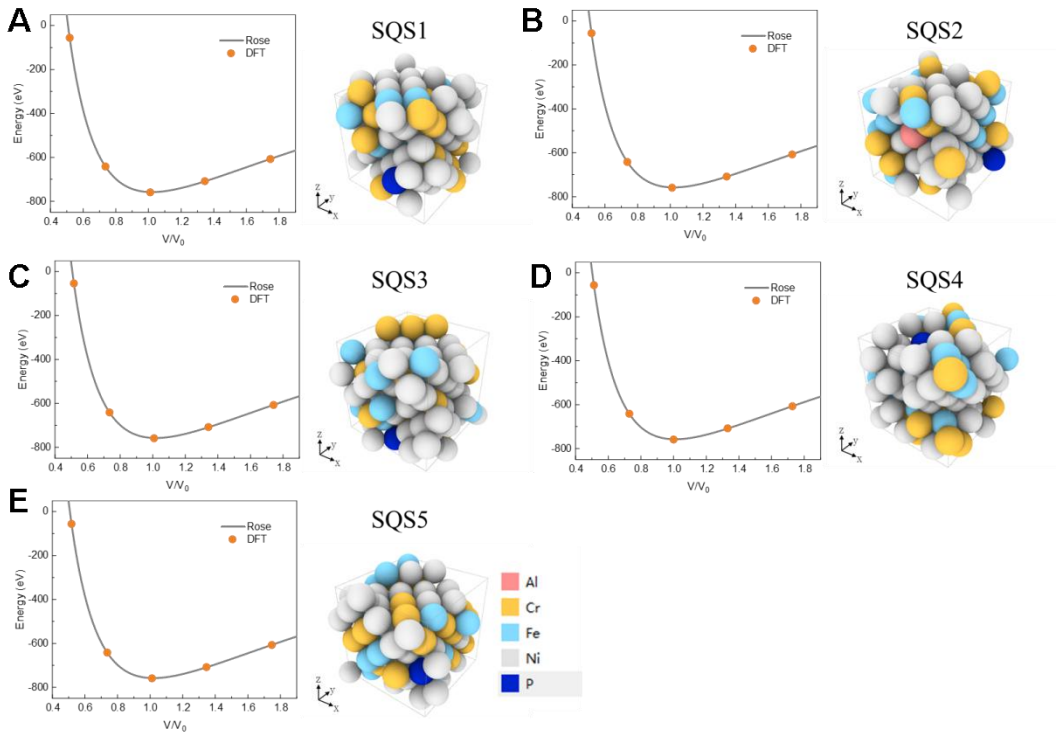

Supplementary Figure 20. Comparison of the energy–volume scaling relationships for the $Ni_{55-x}Cr_{20}Fe_{20}Al_5P_x$ quinary alloy configurations, obtained from the Rose equation and reference DFT calculations. The horizontal axis denotes the relative volume (V/V_0), and the vertical axis represents the energy (eV), demonstrating the general applicability of the Rose equation to multi-component alloys. Panels (A)–(E) correspond to the five quasi-random structures generated by the SQS, respectively. The five structures are FCC with Ni-based, differing only in the distribution of solute atoms.

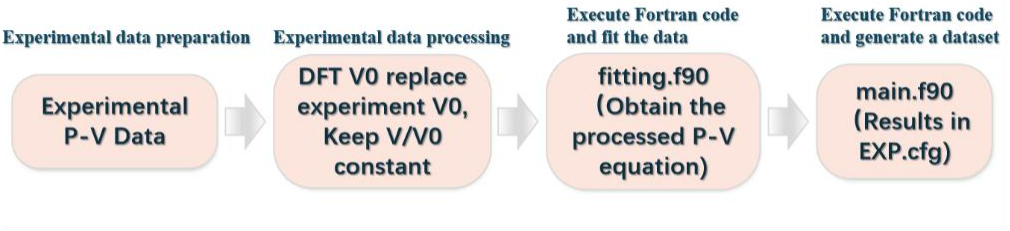

Supplementary Figure 21. PhyMLP fitting experiment procedure.

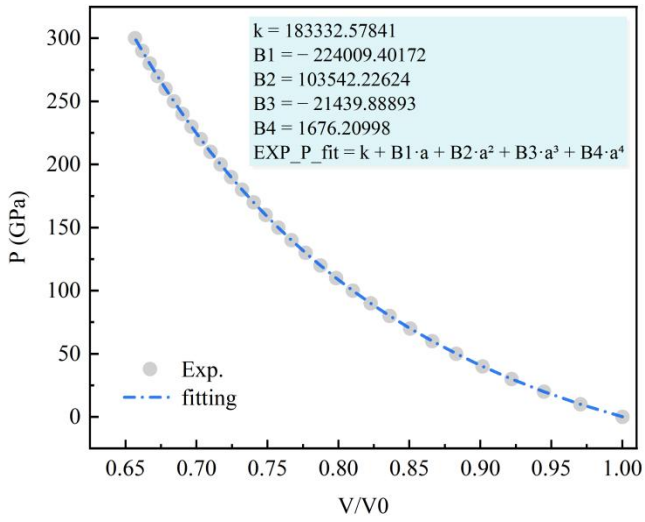

Supplementary Figure 22. Fitting process for P-V relationship.

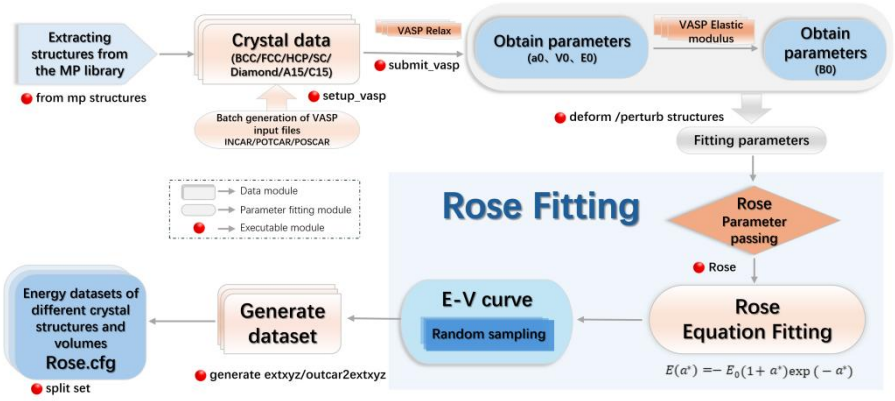

Supplementary Figure 23. Process of acquiring energy data for different crystal structures at different volumes.

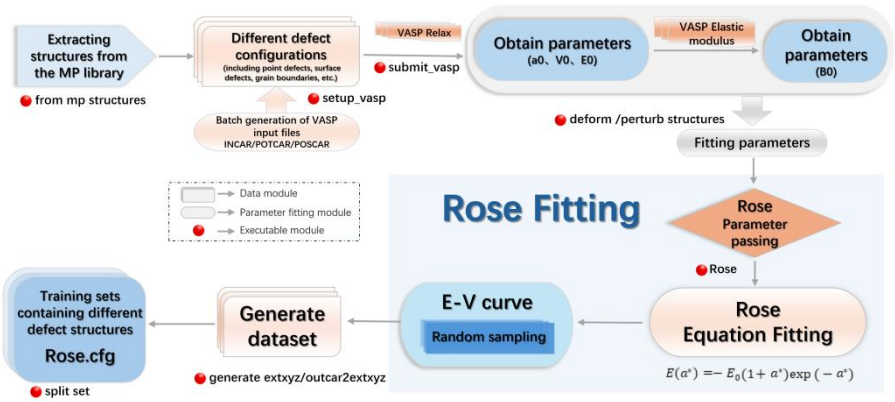

Supplementary Figure 24. Training process with different defect structures.

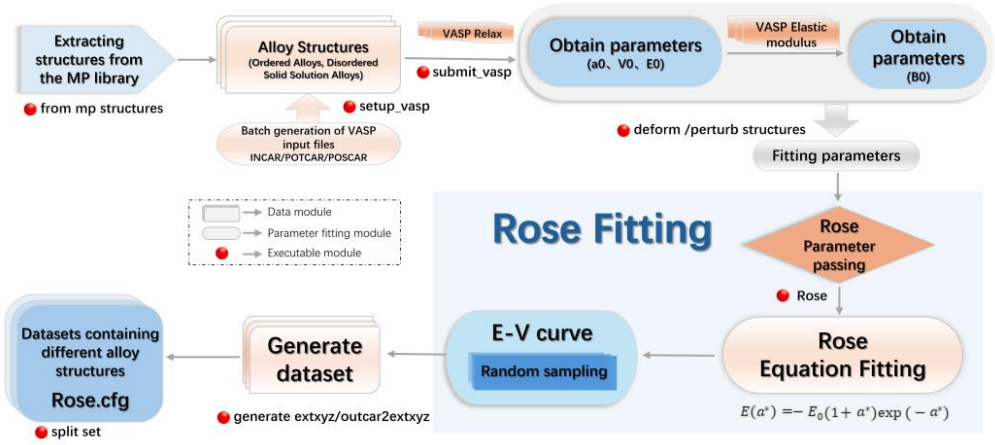

Supplementary Figure 25. Training process for different alloy structures.

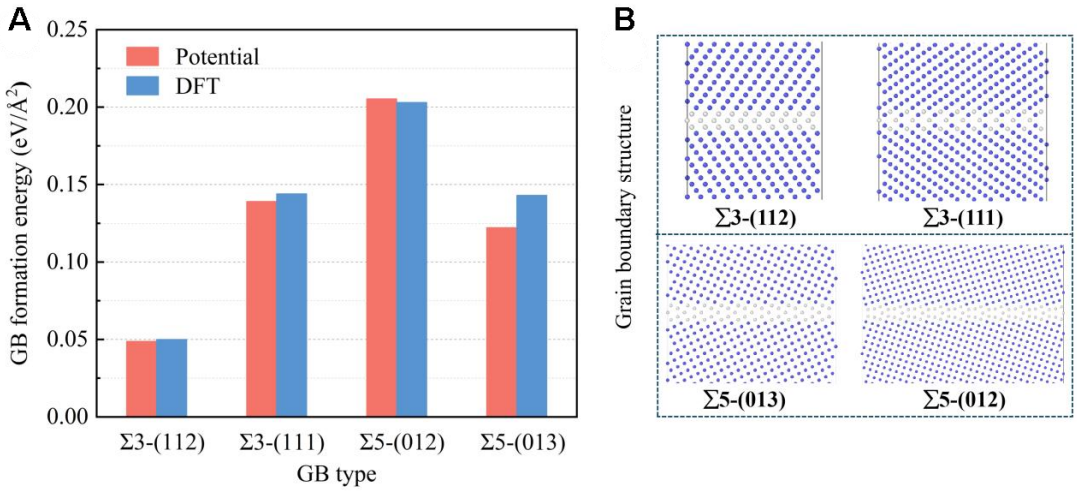

Supplementary Figure 26. (A) Comparison of different grain boundary energies calculated by machine learning tungsten potential function with DFT results, (B) Grain boundary configuration after relaxation.

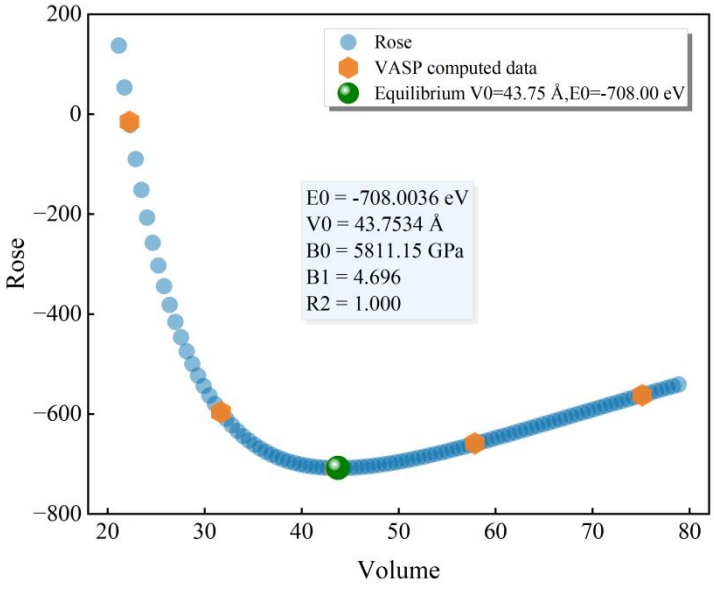

Supplementary Figure 27. Rose equation of state and DFT fitting results.

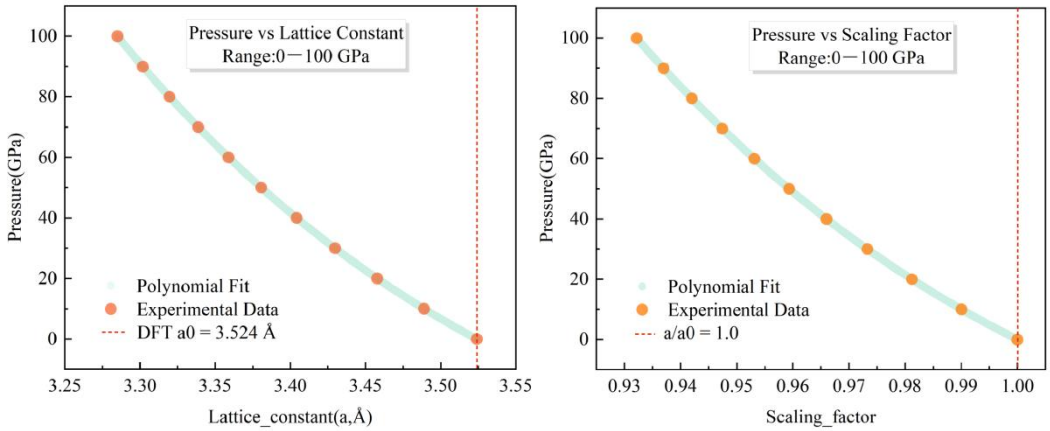

Supplementary Figure 28. Fitted curves and discrete data points in the P-V experimental data extraction module.

Supplementary Table 1. Comparison of point defect properties calculated using tungsten potential function with DFT results and mainstream machine learning potentials

Property	Potential (This work)	DP-HYB-22 [1]	GAP-19 [2]	SNAP-23 [3,4,5]	DFT
E^f_{Vac}	3.21	3.30	3.30	2.61	3.22 [1]
E^m_{Vac}	1.74	1.64	1.70	N	1.73 [2]
$E^b_{Vac-Vac\,(1nn)}$	0.16	N	N	N	0.05 [3]
$E^b_{Vac-Vac\,(2nn)}$	−0.08	N	N	N	−0.29 [3]
$E^f_{<111>d}$	10.23	9.82	10.41	9.63	10.28 [1]
$E^f_{<111>c}$	10.23	N	10.41	N	10.29 [1]
$E^f_{<110>d}$	10.60	10.17	10.62	10.13	10.58 [1]
$E^f_{<100>d}$	11.89	11.82	12.23	10.71	12.20 [1]
E^f_{Oct}	12.27	N	12.35	N	12.27 [1]
E^f_{Tet}	11.94	N	11.75	N	11.72 [1]
$\Delta E_{<111>d-<111>c}$	0.002	N	0.000	N	0.003 [1]
$\Delta E_{<110>d-<111>d}$	0.37	N	N	N	0.30 [1]

[1] Wang X, et al., Nucl. Fusion. 2022;62(12):126013.

[2] Byggmastar J, et al., Phys. Rev. B. 2019;100(14):144105.

[3] Lide DR, et al., BocaRaton: CRC Press; 1999.

[4] Qi X, et al., J Appl. Phys. 2020;128(10):105105.

[5] Renault PO, et al., Appl. Phys. Lett. 1998;73(14):1952.

[6] P.W. Ma, et al., Phys. Rev. Mater. 3 (2019) 013605.

[7] P.W. Ma, et al., Phys. Rev. Mater. 3 (2019) 063601.

[8] D.R. Mason, et al., J. Phys. Condens. Matter. 29 (2017) 505501.